

1
2
3
4
5
6
7 Nanopore-Based DNA Hard Drives for Rewritable
8
9
10
11 and Secure Data Storage
12
13
14
15

16 *Kaikai Chen, Jinbo Zhu, Filip Boskovic and Ulrich F. Keyser**
17
18
19

20
21 Cavendish Laboratory, University of Cambridge, JJ Thomson Avenue, Cambridge CB3
22
23

24 OHE, United Kingdom
25
26
27
28
29
30
31
32
33

34 ABSTRACT
35
36
37
38

39 Nanopores are powerful single-molecule tools for label-free sensing of nanoscale
40
41
42 molecules including DNA, which can be used for building designed nanostructures and
43
44
45 performing computations. Here, DNA hard drives (DNA-HDs) are introduced based on
46
47
48
49 DNA nanotechnology and nanopore sensing as a rewritable molecular memory system,
50
51
52
53 allowing for storing, operating and reading data in the changeable three-dimensional
54
55
56
57
58
59
60

1
2
3 structure of DNA. Writing and erasing data are significantly improved compared to
4
5
6
7 previous molecular storage systems by employing controllable attachment and removal
8
9
10 of molecules on a long double-stranded DNA. Data reading is achieved by detecting the
11
12
13 single molecules at the microsecond timescale using nanopores. The DNA-HD also
14
15
16
17 ensures secure data storage where the data can only be read after providing the correct
18
19
20
21 physical molecular keys. Our approach allows for easy-writing and easy-reading,
22
23
24 rewritable and secure data storage toward a promising miniature scale integration for
25
26
27
28 molecular data storage and computation.
29
30
31

32
33 **KEYWORDS:** Single-molecule, Nanopore sensing, DNA nanotechnology, DNA
34
35
36 nanostructures, Molecular data storage
37
38
39
40
41
42
43
44
45
46
47

48
49 DNA is a natural material for storing genetic information, but it has also been
50
51
52 repurposed as building blocks for creating designed nanostructures with bespoke
53
54
55
56 functionality. Nanoscale structures and patterns can be made by using the self-assembly
57
58
59
60

1
2
3 of single-stranded DNA tiles or by stapling a scaffold DNA strand into a designed structure
4
5
6
7 using complementary short single-stranded oligos.¹⁻³ Traditionally, DNA constructs and
8
9
10 their shape have been characterized using Atomic force microscopes (AFMs),
11
12
13 transmission electron microscopes (TEMs) and optical methods.⁴ For scalable label-free
14
15
16 characterizing a large number of single molecules made from DNA, nanopore sensing is
17
18
19 an ideal method.⁵ Crucially, the ionic current signal of a molecule passing through the
20
21
22 nanopore reveals its 3D shape and thus translates DNA structures into electrical signals.⁶⁻
23
24
25
26
27
28 ⁹ The combination of tailor-made DNA nanostructures with the ease and rapidity of
29
30
31 nanopore analysis of these structures shows great potential for applications in biosensing,
32
33
34
35 molecular machines and molecular data storage.

36
37
38
39 For molecular data storage, the most common approach is to store data in the DNA
40
41
42 sequence by synthesizing DNA strands with designed sequences,¹⁰ with obvious
43
44
45 advantages like high density, high durability and low maintenance costs.¹¹⁻¹⁵ However,
46
47
48
49 synthesis-based DNA data storage relies on creating new DNA strands with unique
50
51
52
53 sequences for writing more data, causing intrinsic disadvantage in the ease and cost of
54
55
56
57
58
59
60

1
2
3 data writing. Besides, DNA with a fixed sequence is hard to modify, creating a serious
4
5
6
7 challenge for data operations and computation akin to classical computer memory. Data
8
9
10 security and privacy are also major concerns of important archival storage. Encryption in
11
12
13 the physical keys using the unique characteristics of DNA molecules will allow for secure
14
15
16
17 storage as the information is only retrievable with the correct key.^{16,17} The flexibility of
18
19
20
21 DNA as a functional material based on Watson-Crick base pairing opens pathways to
22
23
24 address the above questions. Strategies^{18,19} based on DNA nanotechnology were put
25
26
27 forward to make full use of the advantage of the material based on base pairing and
28
29
30
31 toehold mediated strand displacement.²⁰⁻²² For instance, employing existing native DNA
32
33
34
35 strands as a carrier for information provides alternative routes to data storage in direct
36
37
38 DNA sequence, including the DNA punch card method²³ or the catalog DNA method²⁴.
39
40
41
42 Similarly, data can also be stored in the 3D structures of designed DNA objects,^{9,25,26}
43
44
45 opening a new route with the potential of convenient writing and reading as an alternative
46
47
48
49 to the data storage in the DNA sequence.
50
51
52
53
54
55
56
57
58
59
60

1
2
3
4 Here, inspired by the principle of hard disk drive where data is stored and changed by
5
6
7 operating on the sites on the disk, we dramatically improve the utility of DNA
8
9
10 nanostructures to achieve rewritable and secure data storage by adding and removing
11
12
13 molecules in domains along a DNA strand. We name our system DNA hard drive (DNA-
14
15
16 HD), which is easily operated requiring only the mixing of premade molecules. Using our
17
18
19 DNA-HDs, we can write data by attaching molecules on dsDNA and erase data by their
20
21
22 targeted removal. We will demonstrate the full capabilities by a complete writing-erasing-
23
24
25 rewriting cycle in this paper. Also, the data can be easily read with nanopores by passing
26
27
28 the molecules through the nanopores to detect their three-dimensional structure. More
29
30
31 importantly, our system enables data encryption through the use of physical keys. Only
32
33
34 the addition of the correct molecular key sequences enables decoding of the data using
35
36
37 nanopore sensing, allowing for secure information storage on DNA.
38
39
40
41
42
43
44
45

46 We show the principle of our platform in **Figure 1**. The DNA-HD is made by annealing
47
48
49 the 7228 nucleotides (nt) linearized M13mp18 single-stranded DNA (ssDNA) scaffold²⁷
50
51
52 and complementary oligonucleotides (Figure 1a, Table S1 and Materials and Methods in
53
54
55
56
57
58
59
60

1
2
3 the Supporting Information). Oligonucleotides at designed positions are replaced with
4
5
6
7 DNA dumbbell hairpins (introduced in a previous study⁹) or ssDNA overhangs. The DNA
8
9
10 is negatively charged so it can be read out using nanopore sensing by applying a potential
11
12
13
14 to drive individual molecules through the sensing volume, which translate the molecular
15
16
17 structure information into ionic current signals on the microsecond time scale (Figure 1b).
18
19
20
21 We used ~14 nm nanopores in this study with an example of the Scanning Electron
22
23
24 Microscope (SEM) image shown in Figure S1 and characterization details in a former
25
26
27 study⁹. Only unfolded translocation events were retained for further analysis as
28
29
30 introduced in a previous study.²⁸ When measured with our ~14 nm diameter nanopores,
31
32
33
34 a group of DNA dumbbells and a streptavidin molecule can create observable downward
35
36
37 peaks in the ionic current signal but the ssDNA overhang is too small to be detected.²⁹ It
38
39
40
41 has been demonstrated that the velocity of the DNA is nearly constant during the
42
43
44 translocation,³⁰ so we can correspond the peak positions in the signal to the actual
45
46
47
48 positions of the attached molecules on the DNA. We employ the dumbbells at designed
49
50
51 positions as references (REFs) to indicate the start and end of the reading, measure
52
53
54
55 translocation velocity and determine the directionality of the DNA-HD. High ('1') bits are
56
57
58
59
60

created by adding biotinylated oligonucleotides that hybridize to the ssDNA overhangs.

Monovalent streptavidin binds to the biotin and creates an observable signal at the biotinylated site. Thus, we define data as '0' (without the bound streptavidin) and '1' (with bound streptavidin) between the REFs along the DNA-HD.

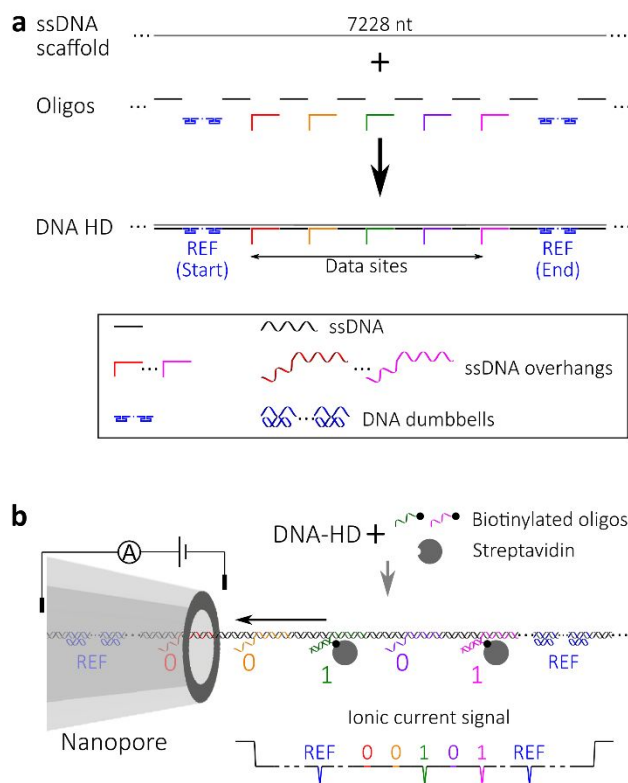


Figure 1. Schematic of the DNA hard drive (DNA-HD). (a) Design of the DNA-HD made

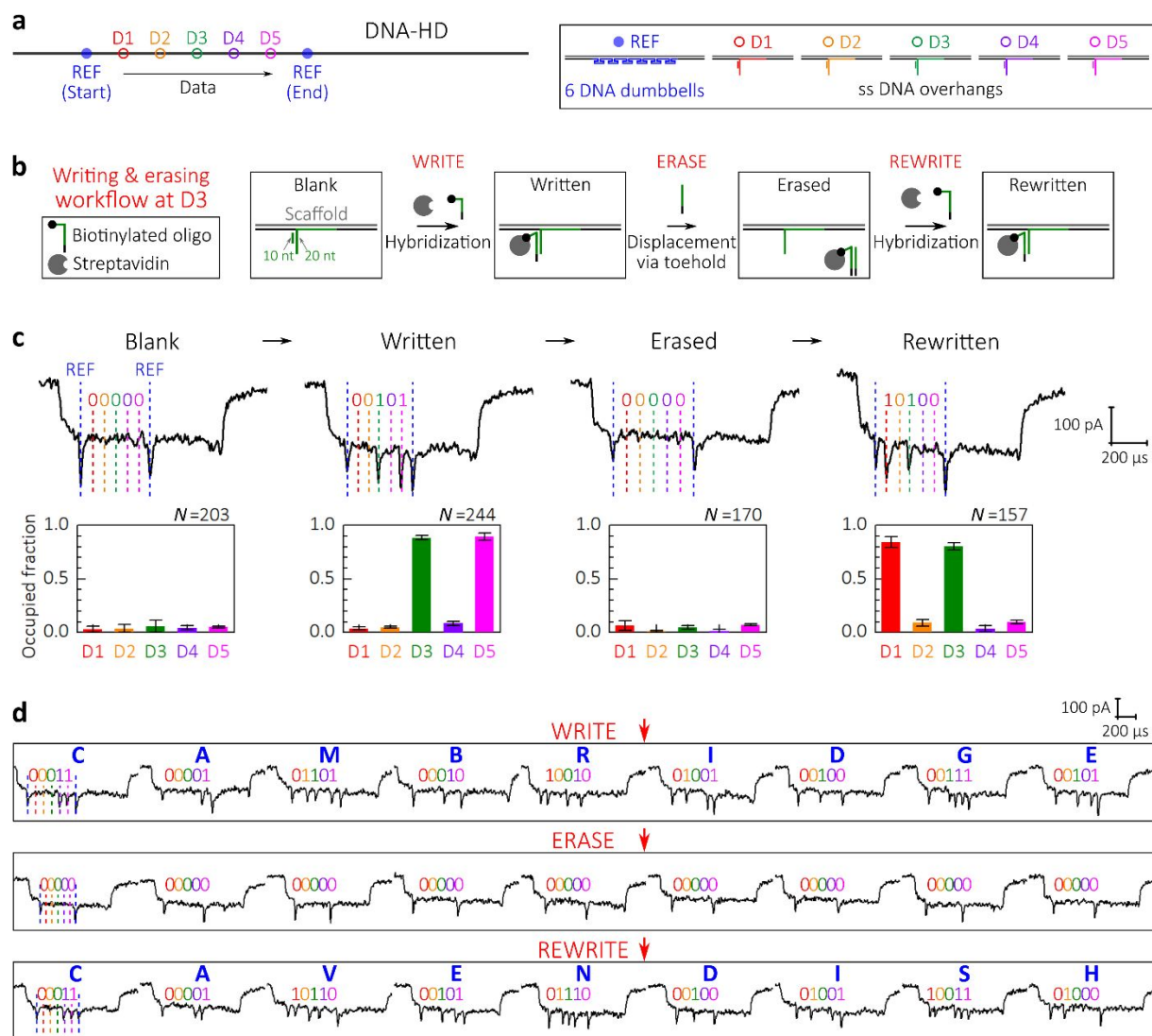
from ssDNA scaffold and designed short DNA oligonucleotides to form units for data

1
2
3 storage and operation. The oligonucleotides assemble to the scaffold via sequence
4
5
6
7 specificity and are designed to incorporate structures like ssDNA overhangs and DNA
8
9
10 dumbbells at designed locations. The legend is shown in the square. (b) Reading the
11
12
13 information on the DNA-HD using a nanopore. Dumbbells are used as fixed references
14
15
16
17 (REFs) to indicate the storage region. Streptavidin and biotin labelled oligonucleotide
18
19
20
21 (complementary to the ssDNA overhang) are added to specifically bind to the ssDNA
22
23
24 overhang to generate detectable signals. Here in the example, only oligonucleotides
25
26
27
28 complementary to the green and magenta overhangs are added, so the two sites are read
29
30
31 as '1' while the others '0'.
32
33
34
35
36
37
38
39
40

41 Based on this platform, we now demonstrate that we can write, erase and rewrite data
42
43
44 on the DNA-HDs to show the rewritable data storage. To facilitate the proof of concept,
45
46
47 the DNA-HD is designed with five sites with ssDNA overhangs between two REF sites
48
49
50
51 (see sequences in Table S2), which we name D1-D5 (**Figure 2a**). REF sites created by
52
53
54 two groups of DNA dumbbells are used to indicate the beginning and end of the data and
55
56
57
58
59
60

1
2
3 determine the direction of DNA-HD according to their predesigned positions. Here, the
4
5
6
7 two REFs are asymmetrically distributed along the DNA. In the current design REFs are
8
9
10 only found in one half of the molecule which allows us to easily extract the translocation
11
12
13 direction from the signal. Figure 2b shows the schematic workflow of the writing and
14
15
16 erasing using D3 as an example. In the initial stage, only a 20 nt overhang partly
17
18
19 hybridized with a 10 nt ssDNA blocking strand is on the DNA-HD, which is classified as
20
21
22 '0'. The 10 nt provides enough specificity to address all the sites individually. Information
23
24
25 is written by hybridizing biotin-labelled ssDNA (Table S3) with the complementary
26
27
28 sequence to the overhang ('WRITE'). After the addition of streptavidin, all biotinylated
29
30
31 sites present now an observable secondary current peak in nanopore measurements
32
33
34 (read as '1'). The biotin-labelled strand includes a free toehold end (black) which is used
35
36
37 to remove the streptavidin carrying strand from the carrier by adding a complementary
38
39
40 strand (Table S3) using a specific strand displacement reaction. The toehold enables the
41
42
43 targeted reset of the bit to '0' ('ERASE'). After erasing of the data, the carrier is ready for
44
45
46 a new biotin labelled strand to be added to store information in a new cycle ('REWRITE').
47
48
49
50
51
52
53
54
55
56 In the above operations, we waited for 1 hour during each procedure (see details in the
57
58
59
60

Experimental Workflow in the Supporting Information) as a demonstration, which can be considerably shortened by optimizing the experimental parameters.^{31,32}



1
2
3 **Figure 2.** Writing and erasing data on DNA-HDs. (a) Design of a writing system on a 7228
4 bp long DNA-HD. Two groups of DNA dumbbells (marked as “REF” in blue) are used as
5
6 references to indicate the start and end of the storage region. Five positions (D1-D5) with
7
8 ssDNA overhangs are designated (sequences are shown in Table S2). (b) Stages of data
9
10 writing and erasing on the DNA-HD using D3 as an example. WRITE: A biotin-labelled
11
12 ssDNA strand is used to write as it binds to the overhang with streptavidin added to cause
13
14 observable signals in the nanopore reading. ERASE: A designed ssDNA strand erases
15
16 D3 by removing the bound biotin-streptavidin using a strand displacement reaction.
17
18 REWRITE: After erasing, new data can be encoded by adding new biotinylated ssDNA
19
20 strand, completing the writing-erasing-rewriting cycle. (c) Characterization of the
21
22 performance of the system. ‘00101’ was written and erased, and then ‘10100’ was written.
23
24
25
26
27
28
29
30
31
32
33
34
35
36
37
38
39
40
41
42
43
44
45
46
47
48
49
50
51
52
53
54
55
56
57
58
59
60

Histograms show the statistics from hundreds of molecules (N is the number of molecules) where the occupied fraction means the per cent of the signals read as ‘1’ on the site out of the total molecule number. See the statistics in Table S4. (d) Demonstration of storing letters as 5-bit ASCII on DNA-HDs and reading the data with nanopores. See the statistics in Table S5.

1
2
3
4
5
6
7
8 We characterized the performance of our method by writing '00101' (D1-D5), erasing
9
10
11 this information and rewriting '10100'. As described above, corresponding
12
13
14 oligonucleotides and streptavidin were added in each step and the resulting molecules
15
16
17 were analyzed with nanopores (see the Experimental Workflow in the Supporting
18
19
20 Information). Figure 2c shows examples of nanopore signals with more events shown in
21
22
23 Figure S2. As each streptavidin label caused a secondary current peak in the event, the
24
25
26 information was decoded by analyzing the presence or absence of peaks. Our results
27
28
29 show a high signal-to-noise (SNR) ratio compared to a recent paper using MoS₂
30
31
32 nanopores for the detection of topological variations on DNA.³³ More importantly, our
33
34
35 signals are consistent and the DNA translocation speed is relatively constant, allowing for
36
37
38 correct decoding of the information using single molecules. We analyzed hundreds of
39
40
41 events and plotted the percentage of detected peaks (named 'occupied fraction') at each
42
43
44 site (Figure 2c and Table S4). Initially, all bits had low occupied fractions at the blank
45
46
47 state. In the first writing stage, D3 and D5 were written as '1' where the occupied fractions
48
49
50
51
52
53
54
55
56
57
58
59
60

1
2
3 were close to 80% while they were below 10% for other sites. After the information is
4
5
6
7 erased, occupied fractions dropped again for all sites to below 10%. In the second writing
8
9
10 stage, occupied fractions for D1 and D3 were also close to 80% and others were below
11
12
13 10%. These significant changes make it possible to correctly detect the information with
14
15
16 high certainty using only a few events. It is noticeable that this error rate is a simple
17
18
19 average from multiple single molecules and includes both writing and reading errors
20
21
22 which can be fully optimized by improving the experimental parameters and analysis
23
24
25 methods. For instance, optimizing the match of nanopore dimensions to the bit size would
26
27
28 increase the signal-to-noise ratio. Variation in the translocation velocity can cause errors
29
30
31 if the bits are not correctly assigned, thus placing reasonable REFs and controlling DNA
32
33
34 velocity by external parameters like electro-osmotic flow, charge or nanopore geometry
35
36
37 will help improve the reading accuracy. Another possibility to reduce errors is to encode
38
39
40 '0' with smaller structures.²⁶ Comprehensive data analysis using multiple molecules and
41
42
43 machine learning will also significantly improve the error rate.^{26,34} After the
44
45
46 characterization, we stored words and changed the data using the designed toehold-
47
48
49 based rewriting capability (Figure 2d). Nine samples were prepared and measured. Here
50
51
52
53
54
55
56
57
58
59
60

1
2
3 we use D1-D5 (corresponding to last 5 bits of ASCII) to encode letters and read them by
4
5
6
7 aggregating the first ten unfolded translocation events for each sample. First, we encoded
8
9
10 'CAMBRIDGE' into the samples with example events and codes shown in Figure 2d
11
12
13
14 (details are shown in Figure S3). Using the same samples, we erased the letters (Figure
15
16
17 S4) and wrote 'CAVENDISH' and measured again (Figure S5). The results show we can
18
19
20
21 encode and change data on the DNA-HDs and read the data with nanopores.
22
23
24

25 The above results show that we can operate on the DNA-HD to achieve rewritable data
26
27
28 storage which can also be adapted to DNA computing as well. In the next step, we show
29
30
31
32 our platform can securely store data by encoding information in the DNA nanostructures
33
34
35 that cannot be directly read but can be decoded by adding required molecules to reveal
36
37
38 the structure information. To this end, we encrypt data on ssDNA overhang sites by
39
40
41
42 applying the requirements of additional complementary sequences labelled with biotin
43
44
45 and streptavidin for correct reading. The biotin-labelled complementary oligonucleotide
46
47
48 serves as a physical key for data access. Using this idea, we designed sites for data
49
50
51
52 encryption on the DNA-HDs (**Figure 3a**) where we included the predesigned parts for
53
54
55
56
57
58
59
60

1
2
3 address (A1-A3) and data (D1-D5) split by the REFs (the REF at the end indicates the
4
5
6
7 direction, see sequences in Tables S6 and S7). The address part is used to identify the
8
9
10 order of the data when we need to store data in different domains in a mixture. Here we
11
12
13 use DNA dumbbells as unencrypted data sites and ssDNA overhangs as encrypted sites
14
15
16 (A3 and D5, Figure 3b), where a blank site (only with ssDNA complementary to the
17
18 scaffold) means a '0' while a group of dumbbells or the ssDNA overhang a '1'. Figure 3b
19
20
21 shows the principle of encryption. For these sites, the address key and data key are the
22
23
24 streptavidin and biotin labelled oligonucleotides complementary to the overhangs at A3
25
26
27 and D5 respectively. The data can be only correctly read after the molecular keys are
28
29
30 bound to the DNA-HD. One typical example is shown (Figure 3c) where we encoded the
31
32
33 word 'SHANNON' (to pay tribute to "the father of information theory") and decoded it with
34
35
36
37
38
39
40
41
42
43
44
45
46
47
48
49
50
51
52
53
54
55
56
57
58
59
60
nanopores. We encoded each letter in the data part of a DNA-HD and the order in the
address, and then made DNA-HDs and mixed them into a mixture. With both address
and data keys presented, we successfully decoded the information with example signals
shown in Figure 3d (analysis in Figure S6). However, when the sample was read without
the keys, the wrong information appeared (Figure 3e, details in Figure S7). First, the order

1
2
3 of the letters could not be correctly aligned without the correct address. Second, the
4
5
6
7 encrypted letters on the HDs were not correctly retrieved due to the unrevealed D5. Based
8
9
10 on this model, the DNA-HDs can be expanded with more address and data sites on each
11
12
13 to encode more practical information. It should be noted that we only show the encryption
14
15
16
17 of one bit on the address and one bit on the data to demonstrate the capability. Using our
18
19
20 platform, we are able to choose any bit, even all the bits, to be encrypted to allow for ultra-
21
22
23 secure data storage. To the best of our knowledge, there is not a straightforward method
24
25
26
27 to decode the information without our physical keys and nanopore sensing platform if all
28
29
30 the bits are encrypted. Even more importantly, the information could not even be retrieved
31
32
33
34 with DNA sequencing.
35
36
37
38
39
40
41
42
43
44
45
46
47
48
49
50
51
52
53
54
55
56
57
58
59
60

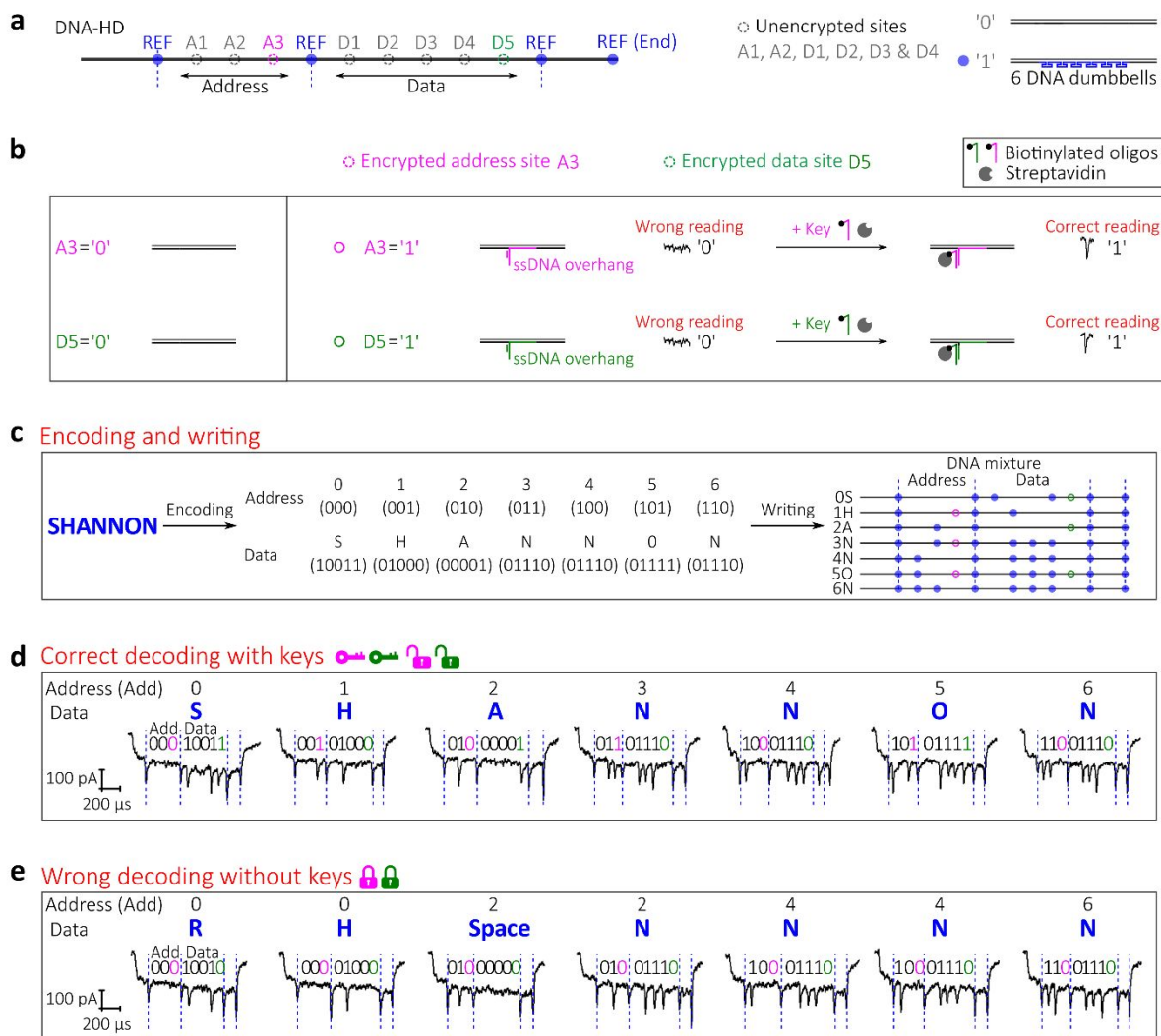


Figure 3. Data encryption on DNA-HDs. (a) Design of the DNA-HD for data encryption with 8 bits used for the example of address and data encoding. Schematics of the unencrypted sites are shown, where blank dsDNA is used to represent '0' and dumbbells '1'. (b) Schematic of the sites for information encryption and the principle of encryption. For these sites, blank dsDNA is used to encode '0' and streptavidin and biotin bound

1
2
3 ssDNA overhang to encode '1'. But the '1' can only be read with the keys (biotin-labelled
4
5
6
7 ssDNA and streptavidin) added. (c) An example of data encryption by encoding
8
9
10 "SHANNON" into a mixture of DNA-HDs. (d) Correct decoding the information with the
11
12
13
14 address and data keys. See detailed data analysis in Figures S5. (e) Wrong information
15
16
17 decoded without keys. See detailed data analysis in Figures S6.
18
19
20
21
22
23
24
25

26 In this study, we demonstrate the original innovation only by showing encoding words,
27
28
29 but our platform can be scaled up by using automated droplet microfluidics in parallel for
30
31
32 writing and parallel nanopore measurement for reading.³⁵ The amplification of these DNA
33
34
35 nanostructures is possible if we optimize the design by using closed ssDNA bulges or
36
37
38 DNA stem loops^{36,37} instead of the open overhangs. Our DNA-HDs hence offer the
39
40
41 potential to copy data including random data access by target amplification.¹⁴ Our
42
43
44 approach indeed has an inherently lower density compared to data storage in the DNA
45
46
47 sequence which is $\sim 10^6$ of that in hard drives.¹⁰ In our previous studies, we have
48
49
50 demonstrated that our nanopore sensing platform can achieve a resolution of around 100
51
52
53
54
55
56
57
58
59
60

1
2
3 bp, meaning that we can store one bit per 100 bp and our data density is already ~3
4
5
6
7 orders of magnitude higher when compared to hard drives.²⁶ However, the resolution of
8
9
10 nanopore for sensing DNA can be significantly improved by using nanopores in thin
11
12
13 graphene³⁸ or MoS₂ membranes³² with thickness below 1 nm. The design of DNA
14
15
16 nanostructures can also be much smaller and more precise to achieve the storage of one
17
18
19 bit of data in tens of base pairs. It should be noted that pushing the limit in data density is
20
21
22 only one aspect for molecular data storage as our demonstrated density is already far
23
24
25
26
27 higher than in conventional hard drives. Synthesis-free and easy writing, convenient and
28
29
30 fast reading, potential for integration and adaptability to variable functions are attracting
31
32
33 and our platform provides a route towards these directions. Our synthesis-free writing
34
35
36 employs only mixing of predesigned building blocks and the nanopore sensing provides
37
38
39 a convenient and fast reading, both can be achieved quickly and easily to be integrated
40
41
42 into miniature scale. Last but not least, our nanostructure consists of double-stranded
43
44
45 DNA (dsDNA) with nicks, so it should be stable enough, at least more stable than complex
46
47
48 DNA nanostructures which can be stored for years,³⁹⁻⁴¹ due to the relative long
49
50
51 hybridization length of 38 bp for each short strand.
52
53
54
55
56
57
58
59
60

1
2
3
4 To conclude, we introduce an approach to store digital information on addressable
5
6
7 molecules along dsDNA, which we name DNA-HD. We employ DNA overhangs as sites
8
9
10 for adding or removing molecules for dynamic data storage. Using the ssDNA overhangs,
11
12
13
14 we can encrypt data on the DNA-HDs, and decode by adding the physical keys which are
15
16
17 the specific biotin labelled complementary oligonucleotides and streptavidin. Without
18
19
20 these keys, one is unable to correctly decode the data. Our method with physical keys
21
22
23
24 and nanopore reading is even secured against direct DNA sequencing. Our enzyme-free
25
26
27
28 method has full potential to be automated in combination with microfluidic systems for
29
30
31 rapid assembly by mixing. In the future, ever-improving methods under development in
32
33
34
35 DNA nanotechnology will undoubtedly improve both writing capabilities and data security.
36
37
38 It is also easier to read secondary structures using nanopores than DNA sequencing, and
39
40
41
42 with our nanopore sensing platform, it only takes microsecond timescale to read data on
43
44
45 one DNA-HD suitable for fast reading. In addition, our system can be used for miniature
46
47
48
49 integration to make end-to-end DNA storage devices.⁴² We assume our method will
50
51
52
53 become a promising route for DNA data storage as a complementary means to the data
54
55
56
57
58
59
60

1
2
3 storage in DNA sequence and possibly also for DNA computing due to the flexibility of
4
5
6
7 our platform.
8
9
10
11
12
13
14
15

16 ASSOCIATED CONTENT

17
18
19

20 **Supporting Information.** The following files are available free of charge: Materials and
21
22
23
24 Methods, Experimental Workflow, Figures S1 to S7 and Tables S1 to S7.
25
26
27

28 AUTHOR INFORMATION

29
30
31

32 **Corresponding Author**

33
34
35

36 *Email: ufk20@cam.ac.uk.
37
38
39

40 **Author Contributions**

41
42
43

44 The manuscript was written through the contributions of all authors. All authors have
45
46
47 given approval to the final version of the manuscript.
48
49
50
51

52 **Notes**

53
54
55
56
57
58
59
60

1
2
3 The authors declare no competing financial interest.
4
5
6
7

8 ACKNOWLEDGMENT 9

10
11 We thank Alexander Ohmann for suggestions on the figures, Jefferey Mc Hugh and Dr.
12 Nicole E. Weckman for critical reading of the manuscript, the lab of Mark Howarth at
13 Oxford University for kindly providing monovalent streptavidin and Boyao Liu from
14 Tsinghua University for some sample preparation. Funding: K.C. and U.F.K. acknowledge
15 funding from an ERC Consolidator Grant (Designerpores no. 647144). J.Z. acknowledges
16 funding from an EPSRC grant (EP/M008258/1). F.B. acknowledges funding from George
17 and Lilian Schiff Foundation Studentship, the Winton Programme for the Physics of
18 Sustainability and St John's Benefactors' Scholarship.
19
20
21
22
23
24
25
26
27

28 REFERENCES 29

- 30
31
32 (1) Rothemund, P. W. Folding DNA to create nanoscale shapes and patterns. *Nature*
33 **2006**, *440* (7082), 297-302.
34
35
36
37
38
39
40 (2) Douglas, S. M.; Dietz, H.; Liedl, T.; Högberg, B.; Graf, F.; Shih, W. M. Self-assembly
41 of DNA into nanoscale three-dimensional shapes. *Nature* **2009**, *459* (7245), 414-418.
42
43
44
45
46
47
48 (3) Ke, Y.; Ong, L. L.; Shih, W. M.; Yin, P. Three-dimensional structures self-assembled
49 from DNA bricks. *Science* **2012**, *338* (6111), 1177-1183.
50
51
52
53
54
55
56
57
58
59
60

1
2
3
4 (4) Schnitzbauer, J.; Strauss, M. T.; Schlichthaerle, T.; Schueder, F.; Jungmann, R.
5
6
7 Super-resolution microscopy with DNA-PAINT. *Nat. Protoc.* **2017**, *12* (6), 1198.
8
9

10
11 (5) Dekker, C. Solid-state nanopores. *Nat. Nanotechnol.* **2007**, *2* (4), 209.
12
13

14
15 (6) Singer, A.; Wanunu, M.; Morrison, W.; Kuhn, H.; Frank-Kamenetskii M.; Meller A.
16
17
18
19 Nanopore based sequence specific detection of duplex DNA for genomic profiling. *Nano*
20
21
22
23 *Lett.* **2010**, *10* (2), 738-742.
24
25

26
27 (7) Plesa, C.; Ruitenber, J. W.; Witteveen, M. J.; Dekker C. Detection of individual
28
29
30
31 proteins bound along DNA using solid-state nanopores. *Nano Lett.* **2015**, *15* (5), 3153-
32
33
34 3158.
35
36

37
38 (8) Bulushev, R. D.; Marion, S.; Petrova, E.; Davis, S. J.; Maerkl, S. J.; Radenovic, A.
39
40
41
42 Single molecule localization and discrimination of DNA-protein complexes by controlled
43
44
45
46 translocation through nanocapillaries. *Nano Lett.* **2016**, *16* (12), 7882-7890.
47
48

49
50 (9) Bell, N. A.; Keyser, U. F. Digitally encoded DNA nanostructures for multiplexed,
51
52
53
54 single-molecule protein sensing with nanopores. *Nat. Nanotechnol.* **2016**, *11* (7), 645.
55
56

1
2
3
4 (10) Ceze, L.; Nivala, J.; Strauss, K. Molecular digital data storage using DNA. *Nat. Rev.*
5
6
7 *Genet.* **2019**, *20* (8), 456-466.

8
9
10
11 (11) Clelland C.T., Risca V., Bancroft C. Hiding messages in DNA microdots. *Nature*
12
13
14
15 **1999**, *399* (6736), 533-534.

16
17
18
19 (12) Church, G. M.; Gao, Y.; Kosuri, S. Next-generation digital information storage in
20
21
22
23 DNA. *Science* **2012**, *337* (6102), 1628.

24
25
26
27 (13) Goldman, N.; Bertone, P.; Chen, S.; Dessimoz, C.; LeProust, E. M.; Sipos, B.;
28
29
30
31 Birney, E. Towards practical, high-capacity, low-maintenance information storage in
32
33
34 synthesized DNA. *Nature* **2013**; *494* (7435), 77-80.

35
36
37
38 (14) Organick, L.; Ang, S. D.; Chen, Y. -J.; Lopez, R.; Yekhanin, S.; Makarychev, K.;
39
40
41
42 Racz, M. Z.; Kamath, G.; Gopalan, P.; Nguyen, B. Random access in large-scale DNA
43
44
45
46 data storage. *Nat. Biotechnol.* **2018**, *36* (3), 242.

47
48
49
50 (15) Erlich, Y.; Zielinski, D. DNA Fountain enables a robust and efficient storage
51
52
53
54 architecture. *Science* **2017**, *355* (6328), 950-954.

- 1
2
3
4 (16) Xiao, G.; Lu, M.; Qin, L.; Lai, X. New field of cryptography: DNA cryptography.
5
6
7 *Chinese Sci. Bull.* **2006**, *51* (12), 1413-1420.
8
9
10
11 (17) Halvorsen, K.; Wong, W. P. Binary DNA nanostructures for data encryption. *PloS*
12
13
14 *One* **2012**, *7* (9).
15
16
17
18
19 (18) Yazdi, S. H. T.; Yuan, Y.; Ma, J.; Zhao, H.; Milenkovic, O. A rewritable, random-
20
21
22
23 access DNA-based storage system. *Sci. Rep.* **2015**, *5*, 14138.
24
25
26
27 (19) Lin, K. N.; Keung, A. J.; Tuck, J. M. Dynamic DNA-based information storage. **2019**,
28
29
30
31 836429. *bioRxiv* <https://www.biorxiv.org/content/10.1101/836429v1> (Accessed:
32
33
34 November 09, 2019).
35
36
37
38 (20) Yurke, B.; Turberfield, A. J.; Mills, A. P.; Simmel, F. C.; Neumann J. L. A DNA-
39
40
41
42 fuelled molecular machine made of DNA. *Nature* **2000**, *406* (6796), 605-608.
43
44
45
46 (21) Seelig, G.; Soloveichik, D.; Zhang, D. Y.; Winfree, E. Enzyme-free nucleic acid
47
48
49
50 logic circuits. *Science* **2006**, *314* (5805), 1585-1588.
51
52
53
54
55
56
57
58
59
60

1
2
3
4 (22) Zhang, D. Y.; Winfree, E. Control of DNA strand displacement kinetics using
5
6
7 toehold exchange. *J. Am. Chem. Soc.* **2009**, *131* (47), 17303-17314.
8
9

10
11 (23) Tabatabaei, S. K.; Wang, B.; Athreya, N. B. M.; Enghiad, B.; Hernandez, A. G.;
12
13
14 Leburton J. -P.; Soloveichik D.; Zhao H.; Milenkovic O. DNA punch cards: Encoding data
15
16
17 on native DNA sequences via topological modifications. **2019**, 672394. *bioRxiv*
18
19
20
21
22 <https://www.biorxiv.org/content/10.1101/672394v3> (Accessed: June 22, 2019).
23
24
25

26 (24) Zakeri, B.; Carr, P. A.; Lu, T. K. Multiplexed sequence encoding: a framework for
27
28
29
30 DNA communication. *PLoS One* **2016**, *11* (4).
31
32
33

34 (25) Chandrasekaran, A. R.; Levchenko, O.; Patel, D. S.; Maclsaac, M.; Halvorsen, K.
35
36
37
38 Addressable configurations of DNA nanostructures for rewritable memory. *Nucleic Acids*
39
40
41 *Res.* **2017**, *45* (19), 11459-11465.
42
43
44

45 (26) Chen, K.; Kong, J.; Zhu, J.; Ermann, N.; Predki, P.; Keyser, U. F. Digital data
46
47
48 storage using DNA nanostructures and solid-state nanopores. *Nano Lett.* **2019**, *19* (2),
49
50
51
52
53 1210-1215.
54
55
56
57
58
59
60

1
2
3
4 (27) Bell, N. A.; Keyser, U. F. Specific protein detection using designed DNA carriers
5
6
7 and nanopores. *J. Am. Chem. Soc.* **2015**, *137*(5), 2035-2041.
8

9
10
11 (28) Chen, K.; Juhasz, M.; Gularek, F.; Weinhold, E.; Tian, Y.; Keyser, U. F.; Bell, N.A.
12
13
14 Ionic current-based mapping of short sequence motifs in single DNA molecules using
15
16
17 solid-state nanopores. *Nano Lett.* **2017**, *17*(9), 5199-5205.
18
19

20
21
22 (29) Kong, J.; Zhu, J.; Chen, K.; Keyser, U. F. Specific biosensing using DNA aptamers
23
24
25 and nanopores. *Adv. Funct. Mater.* **2019**, *29*(3), 1807555.
26
27

28
29
30 (30) Bell, N. A.; Chen, K.; Ghosal, S.; Ricci, M.; Keyser, U. F. Asymmetric dynamics of
31
32
33 DNA entering and exiting a strongly confining nanopore. *Nat. Comm.* **2017**, *8*(1), 1-8.
34
35
36

37
38
39 (31) Yurke, B.; Mills, A. P. Using DNA to power nanostructures. *Genet. Program. Evol.*
40
41
42 *M.* **2003**, *4*(2), 111-122.
43
44

45
46 (32) Morrison, L. E.; Stols, L. M. Sensitive fluorescence-based thermodynamic and
47
48
49 kinetic measurements of DNA hybridization in solution. *Biochemistry*, **1993**, *32*(12),
50
51
52 3095-3104.
53
54
55

1
2
3
4 (33) Liu, K.; Pan, C.; Kuhn, A.; Nievergelt, A. P.; Fantner, G. E.; Milenkovic, O.;
5
6
7 Radenovic, A. Detecting topological variations of DNA at single-molecule level. *Nat.*
8
9
10 *Comm.* **2019**, *10*(1), 1-9.

11
12
13
14
15 (34) Misiunas, K.; Ermann, N.; Keyser, U. F. QuipuNet: convolutional neural network for
16
17
18 single-molecule nanopore sensing. *Nano Lett.* **2018**, *18*(6), 4040-4045.

19
20
21
22
23 (35) Bell, N. A.; Thacker, V. V.; Hernández-Ainsa, S.; Fuentes-Perez, M. E.; Moreno-
24
25
26 Herrero, F.; Liedl, T.; Keyser, U. F. Multiplexed ionic current sensing with glass
27
28
29 nanopores. *Lab Chip*, **2013**, *13*(10), 1859-1862.

30
31
32
33
34 (36) Shirak, A.; Seroussi, U.; Gootwine, E.; Seroussi, E. Sequence motifs capable of
35
36
37 forming DNA stem-loop structures act as a replication diode. *FEBS Open Bio* **2017**, *7*(7),
38
39
40
41 944-952.

42
43
44
45
46 (37) Notomi, T.; Okayama, H.; Masubuchi, H.; Yonekawa, T.; Watanabe, K.; Amino, N.;
47
48
49 Hase, T. Loop-mediated isothermal amplification of DNA. *Nucleic Acids Res.* **2000**, *28*
50
51
52
53 (12), 63.

1
2
3 (38) Garaj, S.; Hubbard, W.; Reina, A.; Kong, J.; Branton, D.; Golovchenko, J. A.

4
5
6
7 Graphene as a subnanometre trans-electrode membrane. *Nature*, **2010**, *467*(7312), 190-
8
9
10 193.

11
12
13
14 (39) Kielar, C.; Xin, Y.; Shen, B.; Kostianen, M. A.; Grundmeier, G.; Linko, V.; Keller,

15
16
17
18 A. On the stability of DNA origami nanostructures in low-magnesium buffers. *Angew.*
19
20
21
22 *Chem. Int. Edit.* **2018**, *130* (30), 9614-9618.

23
24
25
26 (40) Kielar, C.; Xin, Y.; Xu, X.; Zhu, S.; Gorin, N.; Grundmeier, G.; Möser, C.; Smith, D.

27
28
29
30 M.; Keller, A. Effect of staple age on DNA origami nanostructure assembly and stability.
31
32
33
34 *Molecules*, **2019**, *24* (14), 2577.

35
36
37 (41) Zhu, B.; Zhao, Y.; Dai, J.; Wang, J.; Xing, S.; Guo, L.; Chen, N.; Qu, X.; Li, L.; Shen

38
39
40
41 J. Preservation of DNA nanostructure carriers: effects of freeze-thawing and ionic
42
43
44 strength during lyophilization and storage. *ACS Appl. Mater. Inter.* **2017**; *9* (22), 18434-
45
46
47
48 18439.

1
2
3
4 (42) Takahashi, C.N.; Nguyen, B. H.; Strauss, K.; Ceze, L. Demonstration of end-to-end
5
6
7 automation of DNA data storage. *Sci. Rep.* **2019**; *9*(1), 1-5.
8
9
10
11
12
13
14
15
16
17
18
19
20
21
22
23
24
25
26
27
28
29
30
31
32
33
34
35
36
37
38
39
40
41
42
43
44
45
46
47
48
49
50
51
52
53
54
55
56
57
58
59
60

TOC figure

